Long-term stability of lignocellulosic papers strengthened and deacidified with aminoalkylalkoxysilanes

Nathan Ferrandin-Schoffel, Charlotte Martineau-Corcos, Camille Piovesan, Sabrina Paris-Lacombe, Odile Fichet, Anne-Laurence Dupont

Stability of lignocellulosic papers strengthened and deacidified with aminoalkylalkoxysilanes

Nathan Ferrandin-Schoffel,[1,2*] Charlotte Martineau-Corcos,[3,4] Camille Piovesan,[1,2] Sabrina Paris-Lacombe,[1] Odile Fichet,[2] Anne-Laurence Dupont[1*]

[1]*Centre de Recherche sur la Conservation des Collections (CRC, CNRS USR 3224), Muséum National d'Histoire Naturelle, 36 rue Geoffroy St Hilaire 75005 Paris, France*
[2]*CY Cergy Paris Université, LPPI, F-95000 Cergy, France*
[3]*Université Paris Saclay, ILV UMR CNRS 8180, Université de Versailles St-Quentin en Yvelines, 78035 Versailles, France*
[4]*Institut Universitaire de France (IUF), 75005 Paris, France*

[*]*Corresponding authors: nathan.ferrandin-schoffel@mnhn.fr; anne-laurence.dupont@mnhn.fr*
+ 33 1 40 79 53 07

Keywords Strengthening; Lignin; Newsprint paper; Alum-rosin; Mechanical properties; Acidity

Abstract

The durability of paper documents treated with aminoalkylalkoxysilane copolymer (co-AAAS) flexible networks, as deacidifying and strengthenening agents, was studied. To this end, a 1922 lignocellulosic newsprint paper was treated with co-AAASs and characterized. Physico-chemical properties such as pH, chromatism, opacity and mechanical strength were measured shortly upon treatment and several years after. In order to better understand the role of the initial degradation state of the paper and the impact of its constituents other than cellulose (lignin, alum-rosin sizing) on the treatment efficiency, several laboratory papers were added as models. It was shown that alum-rosin sizing contributed to a decrease in pH of the most degraded treated paper over the monitoring time, whereas the strengthening effect was mostly affected by the presence of lignin. In particular, for most papers, after several years, the gain in folding endurance was the lowest in the lignin-rich ones. The breaking length of all the papers increased post-treatment and over time, independently of the paper constituents. This was attributed to the slowly progressing aminoalkylalkoxysilanes polycondensation, on the scale of years, as evidenced by Cross Polarisation – Mass Angle Spinning ^{29}Si solid-state Nuclear Magnetic Resonance.

1. Introduction

A growing number of graphic documents in archives and libraries collections are at risk of rapid decay. Indeed, cellulose, the main biopolymer in paper, undergoes acid-catalyzed hydrolysis, which leads to its depolymerization, one consequence of which is the loss of the material's mechanical

properties. Over time, some papers become so brittle that they do not withstand manual handling without material loss. Papers from the 19th to mid-20th containing a high proportion of groundwood pulp and sized with alum-rosin are often the most degraded [1]. Unbleached woodpulp contains significant amounts of lignin (up to 31%) [2], a biopolymer that releases colored and acidic compounds, mainly through oxidation reactions [3–5], which in turn favor cellulose hydrolysis. Alum-rosin sizing is also a major source of acids in paper [6–8]. In order to counter the acid-catalyzed reactions and retard the degradation, (mass) deacidification treatments have been developed in the second half of the 20th century, some of which are still used in several major libraries worldwide [9,10]. The alkaline additives neutralize the acids and provide an alkaline reserve. The latter acts as a buffer and delays further acid-catalyzed hydrolysis. However, such treatments are not usually applied to very brittle paper records, which are in dire need of mechanical strengthening to revert a rapidly approaching end of lifetime. At present, no commercially available treatment can restore the mechanical properties of brittle papers at the mass scale, and workshop-scale solutions are scarce.

Since 2003 [11], one-pot treatments based on aminoalkylalkoxysilanes (AAASs) are investigated in the laboratory for the purpose of simultaneous deacidification and strengthening of acidic and brittle papers. AAAS monomers bear one or several amine groups (alkaline) that allow both the deacidification and the deposition of an alkaline reserve in the paper, through an optimal adsorption on the cellulosic fibers via hydrogen bonds [12–14]. The mechanical strengthening is assumed to be driven by *in situ* polycondensation of the AAAS in the paper, which forms a polymer matrix intertwined to the paper fibrous network. The first step of the polymerization reaction is the hydrolysis of the AAAS alkoxy groups. This is achieved thanks to the residual water naturally present in the paper and the moisture in the air, with no need to adding water to the treatment solution. The second step is the condensation (hydrolytic and/or alcoholic [15]) of the silanol and alkoxysilane functions, which yields a poly-AAAS with some degree of polymerization (DP). The polycondensation being catalyzed in alkaline conditions [16], the amine functions of the AAAS accelerate this reaction step.

Treatment formulations based on binary mixtures of a trifunctional AAAS (three alkoxy groups), 3-aminopropyltriethoxysilane (AP), and a bifunctional AAAS (two alkoxy groups), the latter being either 3-aminopropylmethyldiethoxysilane (AM) or *N*-(2-aminoethyl)-3-aminopropylmethyldimethoxysilane (DIA), were first developed [17–19]. The purpose was to introduce a flexible copolymer network (co-AAAS) in the paper. The trifunctional monomer AP significantly improves the paper tensile strength, and acts as a cross-linker to the bifunctional monomers AM and DIA. The latter react to form linear molecules, which tend to increase the plasticity and folding endurance mostly (pliability). The treatment is thus versatile, as the monomers, their proportions and concentrations are easy to modify. Moreover, it is a mild treatment as for obvious reasons, when restoring cultural heritage artefacts, the use of harsh chemicals or severe treatment conditions has to be avoided. The application of the treatment can be performed in ambient conditions, either by spray or by immersion, with undiluted or diluted AAASs, preferentially in an organic solvent to avoid cellulose fibers swelling and dissolution of graphic media.

Hexamethyldisiloxane (HMDSO) has been used because it is colorless and non-protic. Additionally, it is the solvent used in the mass scale Battelle process [10,20]. HMDSO is inert and non-toxic and it avoids fiber swelling and bleeding of water-soluble inks, dyes and binders.

Co-AAAS formulations were first applied to a simple model paper made of cotton linters (S2) [17]. Both spray and immersion applications of the treatment were effective. The formation of co-AAAS networks was verified through solid-liquid extractions. An alkaline reserve was introduced, and the paper was considerably strengthened, with an increase in the number of double folds of at least 250% with AP-AM 50-50 (wt%). Co-AAAS treatments were subsequently applied to various lignocellulosic model papers [18,19]. However, the same formulations yielded mixed outcomes, and it was proposed that several constituents in the paper could impact the strengthening. In particular, the presence of alum-rosin sizing and groundwood pulp allegedly hampered the reinforcement, while the impact of the kaolin filler was deemed not noticeable. Co-AAAS formulations were later applied to model papers which had undergone artificial aging beforehand in order to reach a degradation level similar to that of century-old newsprint paper. The strengthening efficiency was lowest for the most severely degraded lignocellulosic papers. An optimized co-AAAS formulation was then to an authentic newsprint paper published in 1922 and succeeded in improving its pH, folding endurance and zero-span tensile strength [19].

The co-AAAS treatments will have a better chance to be used by paper conservators once the strengthening limiting factors linked to paper constituents, and any adverse effect, are understood. For a sustainable application, it is a requisite that the treatment should also be durable. For instance, loss of opacity and yellowing should be limited and change as slowly as possible. To this purpose, the focus of the present work was to evaluate the stability of treated with co-AAAS several years ago, and to understand better the reasons affecting the treatment efficiency. The physico-chemical properties measured were pH, chromatism, opacity, co-axial tensile strength and folding endurance. Papers previously treated with various co-AAAS formulations, and which, by the time of the present study, had naturally aged in ambient conditions during three to seven years since the treatment, were examined. This natural aging period circumvented the need for artificial aging. The data were paralleled with those obtained immediately after the treatment.

2. Experimental

2.1. Chemicals

3-aminopropyltriethoxysilane (AP) (> 98%), 3-aminopropylmethyldiethoxysilane (AM) (97%), *N*-(2-aminoethyl)-3-aminopropylmethyldimethoxysilane (DIA) (97%) and hexamethyldisiloxane (HMDSO) (98%) were purchased from ABCR (Gelest, France) and used as received.

2.2. Paper samples

The paper samples included one newsprint paper dated 1922, and several machine-made modern laboratory papers as models. The model papers were used in their unaged form (undegraded) or were artificially aged (degraded) before the co-AAAS treatment. These untreated samples served as control samples and are henceforth referred to as (t_0) samples. The samples were examined immediately after co-AAAS treatment (called (t) samples) and several years (x) after the treatment (called (t + x) samples), period during which they were stored in stable conditions at 23 °C and 50% relative humidity in a climate chamber. The co-AAAS uptake and the value of x is indicated in Table S1 (Supporting Information file).

2.2.1. Naturally aged newsprint paper

A naturally aged lignocellulosic newsprint paper, "Journal des Fabricants de Sucre", issued September 2nd 1922, was provided by the Bibliothèque Nationale de France. It was called J4. Its constituents and main physicochemical properties are reported in Table 1.

The pulp and fibers source of J4 were determined by microscopic examination and histological staining with Herzberg, Lofton-Merritt and Graff-C solutions [21]. Microchemical tests for rosin and aluminum enabled confirming the presence of alum-rosin sizing in the paper [22]. Kaolin fillers were identified using Attenuated Total Reflectance – Fourier-transform infrared spectroscopy (ATR-FTIR) (Figure S1 in the Supporting Information file) by the two absorption bands around 3690 cm^{-1} and 3620 cm^{-1} (O-H stretch) [23] of kaolinite. The amount of kaolin was determined by measuring the ash content (TAPPI T211 om-02) (Table 1) (two repeat measurements).

2.2.2. Model papers

Table 1. Main constituents, structure and physico-chemical characteristics of the papers.

	S2ua	**C1ua**	**C3ua**	**C4ua**	**J4**
Fibers and pulp	Cotton linters	Cotton linters	GWP/BSP 40/60, softwood	GWP/BSP 80/20, softwood	GWP/UBSP/BSP, softwood, trace of straw
Sizing	None	Alum-rosin	Alum-rosin	None	Alum-rosin
Filler	None	None	Kaolin	Kaolin	Kaolin
Ash content (wt%)	< 0.1	0.8 ± 0.1	13.1 ± 0.1	6.6 ± 0.4	18.1 ± 0.4
Grammage (g m^{-2})	76	80	80	52	58
Thickness (µm)	150 ± 7	159 ± 3	152 ± 5	130 ± 2	61 ± 3
pH	6.62 ± 0.08	5.86 ± 0.11	5.50 ± 0.08	6.21 ± 0.06	4.62 ± 0.01

GWP: groundwood pulp. BSP: bleached sulfite pulp. UBSP: unbleached sulfite pulp.

Four machine made model papers S2, C1, C3 and C4 were chosen based on their fiber constituents, and the presence or absence of kaolin fillers and alum–rosin sizing (Table 1). They had been treated

either in the unaged form or after an artificial aging, where the sheets were suspended individually in a climate chamber at 90 °C and 50% relative humidity (RH) according to TAPPI standard T544 by Piovesan *et al* [19]. The aging had been stopped when the average folding endurance fell under or was equal to 20 double folds, which was reached after different durations for each paper. The aged samples are called S2a, C3a and C4a thereafter to distinguish from their unaged counterparts S2ua, C3ua, C4ua.

2.3. Paper treatment

As the physico-chemical data set at (t) was partial, paper sheets were treated following the same procedure as Piovesan *et al.* [18,19] with minor changes, as indicated below. In particular, for each sample added, care was taken to obtaining a closely similar uptake so as to ensure a relevant intra-sample comparison of the data. The average uptake of the papers at (t) and (t + x) is reported in Table S1 (Supporting Information file). The uptake UP was calculated as follows:

$$UP(wt\%) = \frac{w_a - w_b}{w_b} \times 100 \quad (1)$$

where w_b and w_a are the paper weights before and after treatment, respectively. After treatment, each newly prepared sample was dried for at least 3 h at room temperature, conditioned at 23 °C and 50% RH for 24 h at least (TAPPI T402 sp-03) and weighed.

Unaged model papers (S2ua, C1ua, C3ua and C4ua) were treated by immersion. They were cut in 12 cm × 25 cm sheets, rolled and inserted in glass tubes (Wheaton, 35 mm internal diameter × 147 mm, 144 mL). An immersion period of 30 min allowed obtaining uptakes between 4% and 8% for AP-AM 50-50 (wt/wt) (10 wt% in HMDSO) and AP-DIA 50-50 (wt/wt) (4 wt% in HMDSO).

The artificially aged model papers S2a, C3a and C4a, as well as the newsprint paper J4 (cut along folded lines in 13 cm × 28 cm samples) were treated by spray using an airbrush (Airbrush Hobby Kit, Silverline), either with AP-AM or with AP-DIA mixtures, in 50-50 or 5-95 wt% proportions, without dilution in HMDSO.

2.4. Physico-chemical characterizations

The cold extract pH was measured with a pH-meter (Mettler Toledo MA235) according to TAPPI T509 om-02 standard, adapted to a sample mass of 100 mg (same mass/volume ratio). Two repeat measurements were carried out per paper, and the average reported with the standard deviation.

The pKa values of AM, AP and DIA were determined at 22 °C by acid-base titrations. Each AAAS was diluted in distilled water (0.1 M) and titrated with a 0.1 M HCl aqueous solution (Honeywell). The titration curves (pH as a function of HCl volume) are reported in the Supporting Information file (Figures S2, S3 and S4).

Color and opacity measurements were performed using a hand-held spectrophotometer CM-26dG (Konica Minolta) equipped with an integrating sphere. The configuration adopted was in reflectance

mode (360 - 740 nm spectral range, 10 nm steps), with the specular light component included (SPIN), using a 3 mm diameter measurement aperture. The colorimetric coordinates values L^*, a^* and b^* were calculated in the CIELAB 1976 color space, with the D65 Standard Illuminant and 10° Standard Observer (ISO 5631-2 standard). The opacity values were determined with the C Standard Illuminant and 10° Standard Observer (ISO 2471 standard). The measurements were repeated on five to ten different locations on the samples' surface. The averages are reported with the standard deviations. The color difference was calculated as $\Delta E^* = \sqrt{\Delta L^{*2} + \Delta a^{*2} + \Delta b^{*2}}$.

Prior to mechanical testing measurements, the samples were conditioned according to TAPPI T402 sp-03. The tensile strength measurement (TS) was carried out with an Adamel Lhomargy instrument (DY-20N). Tensile Breaking Length (BL), Elongation at Break (EB) and Young modulus (*Y*) were calculated. BL (km) is the limiting length of a strip of paper of uniform width, beyond which, if such a strip was suspended by one end, it would break of its own weight. It is related to the tensile strength T (kN m^{-1}) according to:

$$BL = 102 \times \frac{T}{R} \quad (2)$$

where R is the grammage of the paper (g m^{-2}) (TAPPI T494 om-01 standard).

Folding Endurance (FE) was determined with a Tinius Olsen instrument (applied tension: 500 g) according to TAPPI T511 om-02 standard. FE is reported as the average number of double folds before breaking (N(FE)). For both TS and FE, ten measurements were done per sample in the machine direction of the sheets. Average values are reported with the standard deviations.

The static contact angle measurements were carried out in air at room temperature with a DSA-P instrument (Kruss, Germany). A drop of water (10 µL – Millipore ultrapure) was added on the surface of the paper. The static contact angles were measured from Young-Laplace drop profile fittings. The measurements were carried out in ten different locations. Average values are reported with standard deviations.

The $^{1}H \rightarrow ^{29}Si$ cross-polarization (CP) under magic-angle spinning (MAS) NMR spectra were recorded on a NEO Bruker 500 WB NMR spectrometer (11.7 T). The papers were cut in small pieces and introduced in 4 mm outer diameter zirconia rotors. A 4 mm double resonance probe was used, and all samples were spun at 10 kHz MAS frequency. For the CP transfer, the radiofrequency fields applied on ^{1}H and ^{29}Si channels were 50 kHz and 60 kHz, respectively. The contact time was set to 4.0 ms and the recycle delay to 4 s. ^{1}H decoupling was applied during signal acquisition. Between *ca* 22 000 and 140 000 transients were accumulated per sample (between 1 and 9 days experimental time). The ^{29}Si chemical shifts are externally referenced to TMS at 0 ppm. The spectrum deconvolutions were performed with the Dmfit software [24], using simple Lorentzian/Gaussian line shapes.

3. Results and discussion

Chromatism, opacity, pH and mechanical properties measurements were performed on J4 at (t) and (t + 3). A comparison with the data obtained at (t) and (t + x) for the model papers treated with AP-AM and AP-DIA was made. The aim was to investigate which parameters (paper constituents and/or degradation state) are the limiting factors to the treatment efficiency after several years. Therefore, the impact of the papers' degradation state on the treatment efficiency was examined closely.

3.1. pH change

At (t), both AP-DIA 50-50 and AP-DIA 5-95 raised the pH of J4 to values above 7 (7.27 and 7.55, respectively) (Figure 1a). However, after 3 years, the pH decreased to 6.19 (AP-DIA 50-50) and 6.11 (AP-DIA 5-95). In order to investigate the cause of the pH decrease, the results were paralleled to those obtained for the unaged and aged model papers treated with AP-DIA 50-50 (Figure 1b). These papers show a similar natural aging after treatment (between 4 and 5 years) (Table S1 in the Supporting Information file). In contrast to J4, the pH of most model papers did not decrease with natural aging after treatment, to the exception of C3a, even though its pH did not fall below 7. For the other model papers, except for C3ua, the pH at (t + x) was slightly higher than the value measured at (t). Even though much care was taken in the sample preparation, these slight variations were attributed to the small disparity in the uptakes between (t) and (t + x) since, as explained above, some of the (t) samples were prepared *de novo* (Table S1 in the Supporting Information file). Incidentally, this observation also indicates that the pH is strongly correlated to the uptake, an issue that will be examined further on.

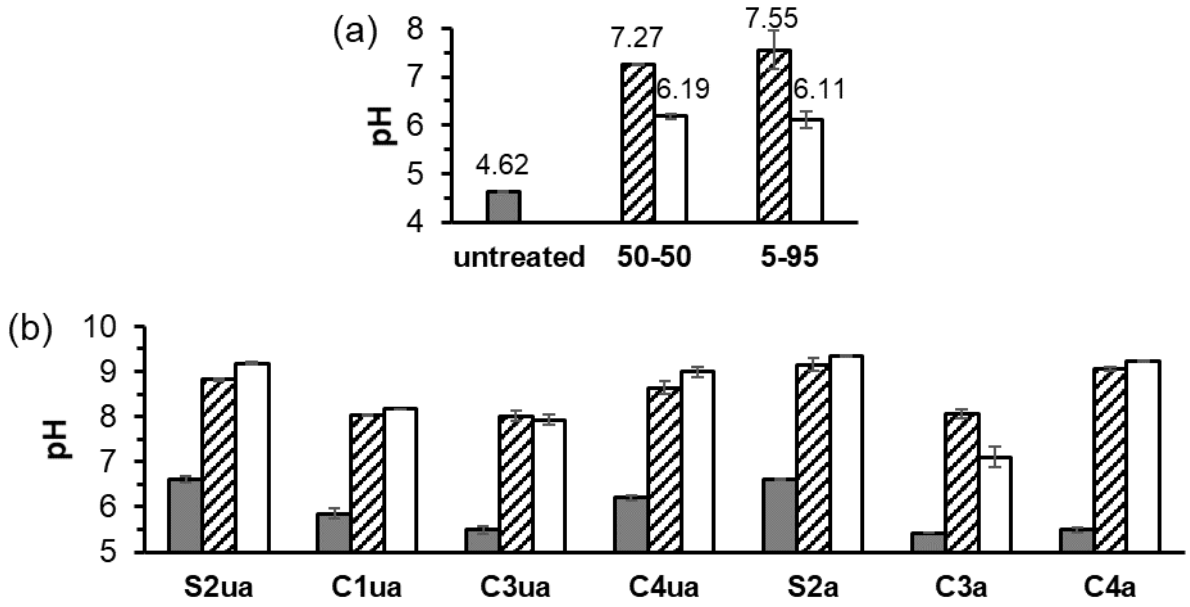

Figure 1. Cold-extract pH of (a) J4 treated with AP-DIA (50-50 and 5-95) and (b) the model papers (unaged and aged) treated with AP-DIA 50-50. Grey filled bar: untreated papers (t_0). Hatched bars: treated papers at (t). White bars: treated papers at (t + x) (x and UP are in Table S1).

Several years after treatment, in stable ambient conditions, none of the papers showed a pH below 6, which is a satisfactory outcome. With AP-DIA 50-50, the decrease in pH of C3a was similar to that of J4 (0.96 and 1.08 units, respectively), and this decrease occurred approximately over the same period (4 and 3 years, respectively). In addition, at (t_0), the pH of C3a (pH = 5.43) was close to the pH of C3ua (pH = 5.50) and the pH of C4a (pH = 5.49). Thus, the decrease in pH that occurred over time after treatment seems unrelated to the pH of the control papers. Furthermore, since the proportion of GWP in C4 is higher than in C3 (about 80% and 40%, respectively, see Table 1), a higher lignin content had most likely no major impact either on the post-treatment pH decrease. Additionally, because neither C4ua nor C4a showed a decline in pH, a high lignin content does not seem to consume the alkaline reserve over time, and hence cannot explain the fall in pH of J4 and C3a.

Another commonality between J4 and C3, also shared with C1, is the alum-rosin sizing. However, in contrast, no decrease of pH was observed for C1ua and C3ua at (t + x). Therefore, a probable cause could be the artificial aging underwent by C3a. The conditions used (temperature, RH) possibly affected the sizing and increased its acidification speed. As the rosin softening point is between 40 °C and 60 °C [25], the rosin in the model papers aged at 90 °C for several weeks may have undergone physicochemical changes. Thus, the rheology of the sizing in paper could have changed during the artificial aging. As J4 has been stored for a century in unknown conditions of temperature and RH, the rosin may have been affected as well.

Alum and rosin are both sources of acidity (and degradation) in paper. Rosin favors the acid hydrolysis of cellulose as it contains acidic terpenoids, including abietic acid and dehydroabietic acid [26]. During the sizing process, rosin is first dissolved in an alkaline aqueous solution through an acid-base reaction with either sodium carbonate or sodium hydroxide [27,28], leading to the formation of amphiphilic salts. Alum (aluminum sulfate) is then used to precipitate the rosinate, which forms a film bonded to the cellulose fibers through electrostatic interactions [28]. To ensure a good binding, the stoichiometry used usually favors an excess of alum, which then stays in the fibers. In the presence of water, aluminum sulfate undergoes hydrolytic decomposition, forming aquo complexes and releases protons [27]. This occurs during natural aging but could also be accelerated during the artificial aging. In conclusion, alum is thought to play a major role in the increase of the acidy of the most degraded papers that were treated with co-AAAS.

The absolute pH variation (ΔpH) as a function of the uptake for the model papers and J4 treated with AP-DIA 50-50 at (t) and (t + x) is shown in Figure 2a. As the alkalinity increases with the uptake [17], all the points at (t) (triangles) fall along a trendline. The data points at (t + x) (circles) follow this trendline as well, to the exception of J4 and C3a (circled data points in Figure 2a), which fall distinctly below. The pH decrease indicates that regardless of the small inter-sample variations in the uptake, the alkaline reserve introduced by the amines was consumed over time in a larger proportion for J4 and C3a than for the other papers, which supports the observations made above about the increase of the acidity. The same was true for the papers treated with AP-AM 50-50 (Figure 2b). J4 and C3a are also distinctly

below the trendline at (t). As mentioned above, both J4 and C3 contain groundwood pulp and are sized with alum-rosin. This supports the fact that, as foreseen, among the model papers, C3 is the most relevant to model J4. This is all the more applicable for the aged sample C3a, in particular because of its low FE value (N(FE) = 14), close to that of J4 (N(FE) = 17) (section 3.4), which indicates a closely matching mechanical degradation state.

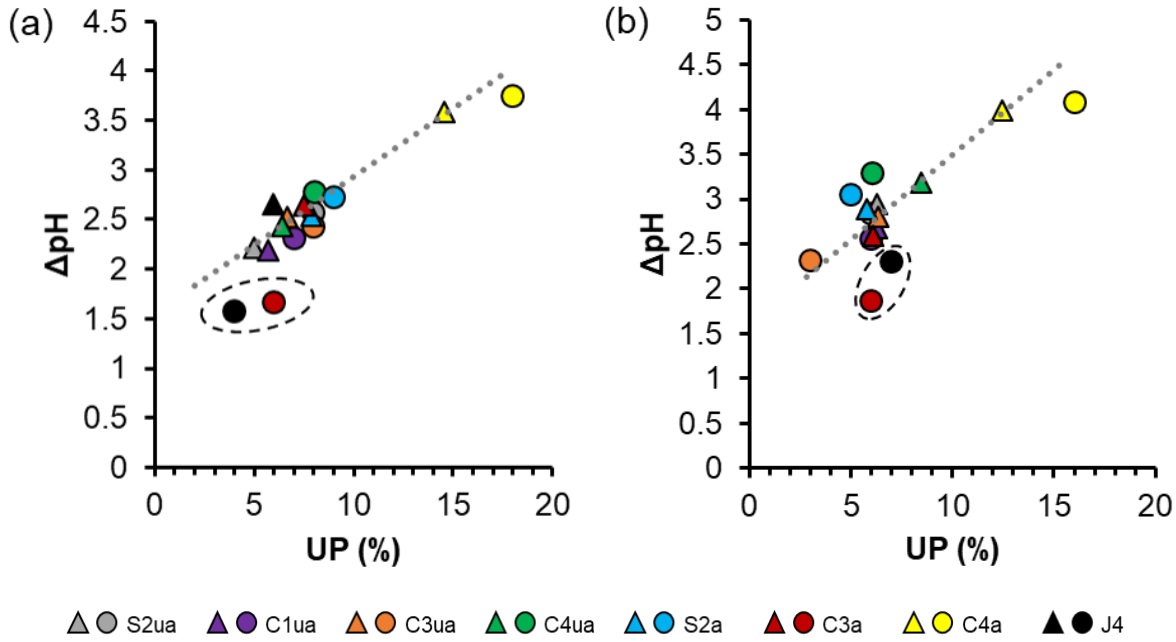

Figure 2. Absolute pH variation (ΔpH) as a function of the uptake (UP) for the papers treated with (a) AP-DIA 50-50 and (b) AP-AM 50-50. Triangles: treated papers at (t). Circles: treated papers at (t + x) (x is in Table S1).

Although DIA bears two amine groups and AM only one, the DIA-based treatments led to pH values close to those obtained with the AM-based treatments (Figure S5 in the Supporting Information file). To investigate this further, the pKa values of the AAAS were measured at 22°C, which yielded pKa(AM) = 10.4, pKa(AP) = 9.7, pKa_1(DIA) = 10.0 and pKa_2(DIA) = 7.0 (Figure S2, S3 and S4 in the Supporting Information file). The low pKa (pKa_2 = 7.0) of one of the amines of DIA indicates that its role in the pH of the DIA treated paper is low. The neutralization and alkaline buffering by DIA are then performed largely by the other amine (pKa_1 = 10.0). On the other hand, the pH at (t) of the papers treated with AP-DIA 50-50 and AP-DIA 5-95 being similar, it was concluded that the slight pKa difference between AP (pKa = 9.7) and DIA (pKa_1 = 10.0) had no major impact on the deacidification.

As pKa of AM is higher than both pKas of DIA, ΔpH at (t) of the model papers treated with AP-AM and AP-DIA were compared. It is then congruent that, when treated with AP-AM to similar uptakes (Table S1), S2ua, C1ua, C3ua, C4ua, S2a and C4a showed higher ΔpH values (ΔpH = 2.94, 2.68, 2.80, 3.19, 2.89 and 3.98, respectively) than when treated with AP-DIA (ΔpH = 2.21, 2.18, 2.52, 2.44, 2.64 and 3.58, respectively). In addition, pH at (t + x) of the papers which had the nearest uptakes was

compared, namely S2ua (UP = 6% for AP-AM, UP = 8% for AP-DIA), C1ua (UP = 6% for AP-AM, UP = 7% for AP-DIA) and C3a (UP = 7% for AP-AM, 6% for AP-DIA). In each case, the pH was higher with AP-AM (pH = 9.46, 8.42 and 7.30, respectively) than with AP-DIA (pH = 9.19, 8.17 and 7.10, respectively), for equal and even slightly longer natural aging duration x (Table S1 in the Supporting Information file). This result indicates that at (t), AP-AM deacidifies more efficiently than AP-DIA, a benefit that lasts until (t + x). This result is counterintuitive if one considers that, due to the presence of two amine groups, DIA should be a better deacidifying agent. Nonetheless, the alkaline pH obtained with the two formulations indicates that both AM and DIA provide a sustainable deacidification.

3.2. Color and opacity changes

Deacidification treatments can induce some yellowing of the paper [10,29], and this could be considered as a drawback by conservators. For a sustainable application of the AAAS, yellowing, as well as loss of opacity or optical modification of the printing media, should be limited, if not absent. As a first observation, none of the treatments did modify the optical properties of the printing inks. No bleeding was observed after adding the AAAS, which confirms earlier findings [30]. The values of b^* and opacity after co-AAAS treatments were measured (Figures 3 and 4).

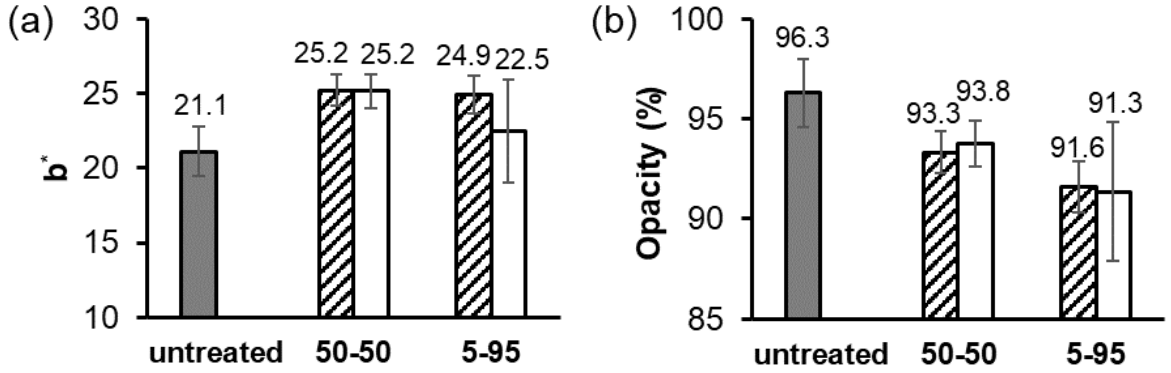

Figure 3. (a) b^* and (b) opacity of J4 treated with AP-DIA (50-50 and 5-95). Grey filled bar: J4 untreated (t_0). Hatched bars: J4 treated at (t). White bars: J4 treated at (t + 3) (UP is in Table S1).

For J4 treated with AP-DIA (50-50 and 5-95), yellowing and loss of opacity were observed after treatment. With both formulations, at (t), $\Delta b^* \approx +4$ (Figure 3a), whereas the opacity decreased by 3.0 points for AP-DIA 50-50 and by 4.7 points for AP-DIA 5-95 (Figure 3b). This loss of opacity is not trivial, yet not unacceptable, considering that the final values were still above 91%, indicating high opacity. The total chromaticity change ΔE^* of the samples comparing (t) to (t_0) was 5.6 for AP-DIA 50-50, and 4.1 for AP-DIA 5-95. This chromatic change is perceptible with the naked eye, considering that the Just Noticeable Difference (JND) in the 1976 CIELAB color space has been defined as $\Delta E^* \approx 2$ [31]. The values of b^* and opacity of the samples treated with either formulation were stable or were not

significantly different for the samples at (t + x). This indicates that in J4 the optical modifications fully occurred immediately after treatment (t).

Recently, the organic reactions likely occurring between the AAAS and the biopolymers in paper were studied using model compounds [32]. Among other reactions, the formation of yellow compounds such as Schiff bases and glycosylamine was identified. The immediate yellowing observed for the treated papers can therefore be explained by the fast reaction between the amine groups of AAAS and specific functional groups on cellulose, hemicelluloses and lignin, as well as their degradation products in the paper, leading to the formation of yellow compounds, among other compounds.

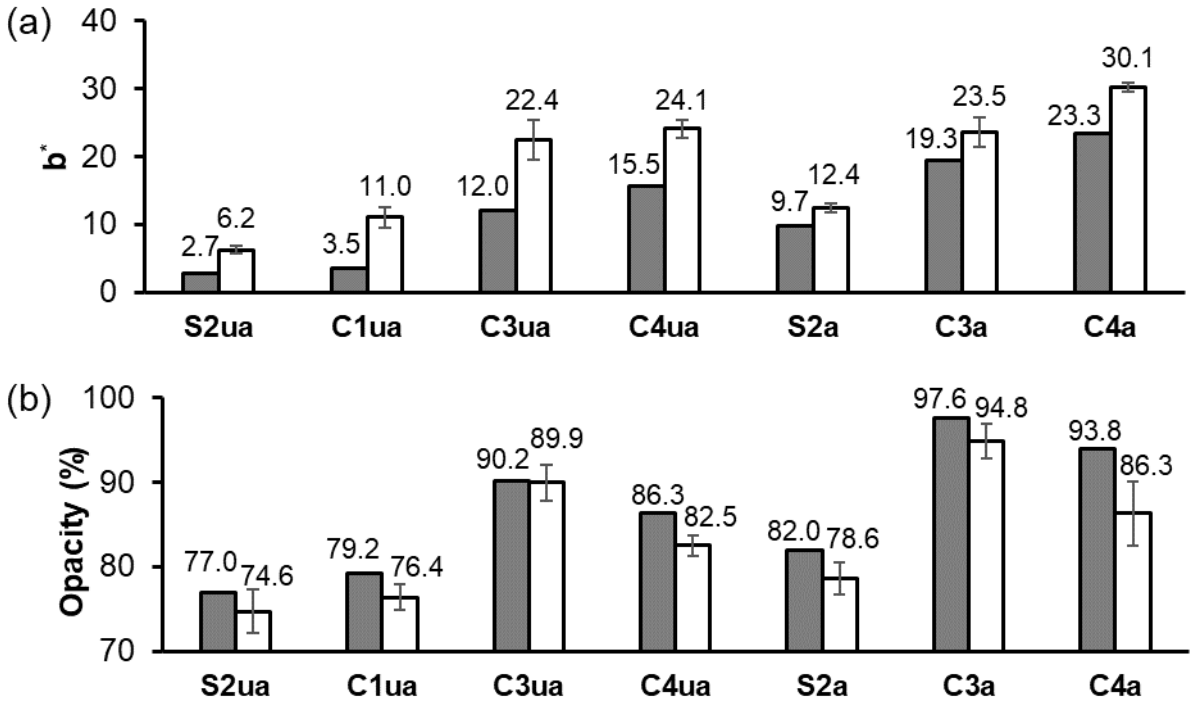

Figure 4. (a) b^* and (b) opacity of the model papers (unaged and aged) treated with AP-DIA 50-50. Grey filled bar: untreated papers (t_0). White bars: treated papers at (t + x) (x and UP are in Table S1).

Opacity and b^* values for the model papers at (t_0) and at (t + x) treated with AP-DIA 50-50 are reported in Figure 4. Yellowing of all the treated papers was observed. Opacity loss was observed too, except for C3ua. Δb^* values (difference in the data between (t_0) and (t + x)) for S2ua (+ 3.5, UP = 8%), C1ua (+ 7.5, UP = 7%), C3ua (+ 10.4, UP = 8%), C4ua (+ 8.6, UP = 9%), S2a (+ 2.7, UP = 9%), C3a (+ 4.2, UP = 6%) and C4a (+ 6.8, UP = 19%) were all above JND (Figure 4a). The slightest yellowing was observed for S2 (S2ua and S2a). As S2 is made of cotton linter (lignin-free pulp) and is unsized, the lignin in C4, the alum-rosin sizing in C1, and the presence of both in C3, were suspected as possible causes of the yellowing observed at (t + x). This can occur through reactions of these paper constituents with the AAASs, as proposed above. Indeed, rosin contains oxidized terpenoids [26], and lignin and its degradation products bear numerous carbonyl groups [3]. These oxidized groups can lead to the formation of Schiff bases through reaction with the AAAS amine moiety.

The loss of opacity in connection with lignin and alum-rosin was less straightforward (Figure 4b). The decrease was the highest for C4a (loss of 7.5 points). However, this result was not attributed to the paper constituents, but mainly to the fact that C4a had the highest uptake (UP = 17%), inducing a larger modification of the physical interactions of the paper with light.

Paper's opacity is largely related to the amount of fillers. In addition to increasing the whiteness and brightness of paper, kaolin is also used to increase its opacity [33]. It is thus congruent that J4 and C3, which have the highest amount of kaolin (ash content of 18.1 wt% and 13.1 wt%, respectively) are the most opaque papers, whereas S2 and C1, which have no fillers, have the lowest opacity values (Figure 4b). Nevertheless, the relation between the amount of kaolin and the decrease in opacity after treatment was unclear. For instance, at similar paper density (similar thickness and grammage), the opacity loss of C1ua and C3a treated with AP-DIA 50-50 to similar uptakes (UP = 7% and UP = 6%, respectively) was the same (Δopacity = 2.8%), despite the fact that C3 contains kaolin and C1 does not. Moreover, as the ash content of C3ua and C3a was the same, no loss of kaolin occurs during aging. As the decrease in opacity occurred for C3a and not for C3ua, the variations could not be attributed to the amount of kaolin. Hence, the larger contributor to the opacity variations seems to be the treatment itself.

AP-AM 50-50 induced yellowing of all the model papers as well (Figure S6a in the Supporting Information file). Again, the smallest Δb^* was obtained for S2 ($\Delta b^* = +2.2$ for S2ua and $\Delta b^* = +0.8$ for S2a), which supports the discussion above on the role of alum-rosin sizing and lignin in the color change. S2ua and C3ua were the only papers to show no decrease in opacity, with even a slight increase for C3ua (Figure S6b in the Supporting Information file). Because of the slight variations in the uptake from one treated paper to the other, Δb^* and Δopacity (absolute values) were plotted as a function of the uptake for both AP-AM 50-50 and AP-DIA 50-50 formulations (Figure S7 in the Supporting Information file). A trend between these changes and the uptake appeared but less clearly, and whether AP-AM or AP-DIA led to larger variations was not obvious.

For J4 treated with AP-DIA 50-50, between (t_0) and ($t + 3$), $\Delta b^* = +4.1$, and the loss of opacity was of 2.5 points (Figure 3). These values were similar to those of C3a ($\Delta b^* = +4.2$, loss of opacity of 2.8%, Figure 4), for similar uptake (J4: UP = 5%, C3a: UP = 6%) and similar aging duration x (C3a: x = 4). The fact that J4 and C3 were both alum-rosin sized and contained groundwood pulp corroborates the hypothesis formulated above about the impact of alum-rosin and lignin on the visual changes. On the other hand, as with AP-AM treatment, no connection between the amount of fillers and the decrease in opacity could be established.

As with pH, the variations in yellowing and loss of opacity over time of J4 and C3a were similar. This confirms that, as reported above, the artificially aged C3 (C3a) appears yet as the most relevant paper to model the naturally aged lignocellulosic newsprint J4. In order to understand and confirm this result, the mechanical properties of the treated papers were characterized. Prior to this, as the mechanical properties of polymers and composites strongly depend on their degree of polymerization [34], the polycondensation state of the AAAS in the paper was studied.

3.3. Progress of the polycondensation

The polycondensation rate of DIA was closely examined. Previously, Souguir *et al.* used ^{29}Si CP-MAS NMR to estimate the number-average degree of polymerization ($\overline{DP}_n$) of the homopolymers AM and DIA in S2ua at (t) [13,14]. In both cases, a low $\overline{DP}_n$ (around 10) indicated that small oligomers were formed. Numerous silanol groups (-Si-OH) should then be present at the end positions, the latter being able to form hydrogen bonds with cellulose and water molecules [35,36]. The small $\overline{DP}_n$ at (t) is confirmed by the gain in hydrophilic character of the treated papers. Indeed, water contact angle measurements could not be performed, as the water drop was absorbed in all the treated papers in a few seconds, including the alum-rosin sized ones which are otherwise hydrophobic (J4 (94.3° ± 8.6°), C1 and C3). Daher *et al.* made similar observations with polyurethane foam, which became more hydrophilic when treated with AM [37]. They proposed the formation of hydrogen bonds between water molecules and the amine functional groups on the AAAS.

Siloxane chains with higher $\overline{DP}_n$ should decrease the number of silanol groups and lead to a progressive increase of the hydrophobic character of the paper. This assumption was confirmed at (t + x) as the water drop remained on the surface of all the papers (unsized and sized). For J4 treated with AP-AM and AP-DIA, static water contact angle at (t + 3) was 102° ± 4 and 83° ± 8 for the 50-50 proportion, and 102° ± 4 and 90° ± 5 for the 5-95 proportion, respectively. Thus, the polycondensation would have progressed slowly with time. In order to confirm this hypothesis, ^{29}Si CP-MAS NMR was carried out on J4 treated with AP-DIA 5-95 at (t) and (t + 3) (Figure 5).

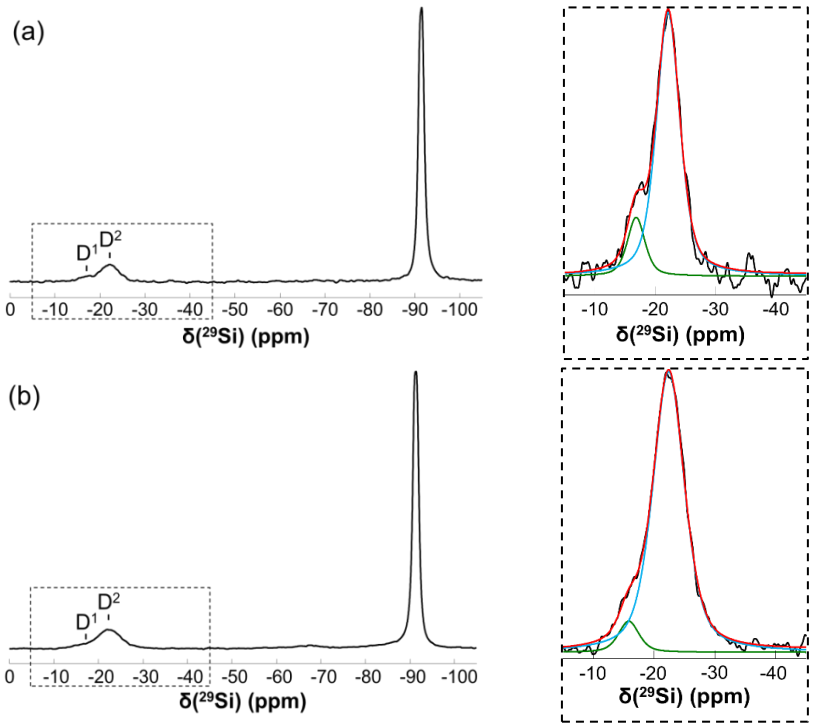

Figure 5. Left: ^{29}Si CP-MAS NMR spectra of J4 treated with AP-DIA 5-95 at (a) (t) and (b) (t + 3). Right: expansions of the area of interest, with the resonance deconvolutions. The red spectrum is the sum of the D^1 (green) and D^2 (blue) contributions.

On both spectra, the two peaks overlapping at about – 16 ppm and – 22 ppm were related to D^1 (silicon atom bonded to one –O-Si group) and D^2 (silicon atom bonded to two –O-Si groups), respectively [14,38]. A third intense signal was visible at about – 91 ppm, which corresponds to the ^{29}Si NMR signal of kaolinite (aluminosilicate) [39] used as a filler in J4. There was no D^0 signal (characteristic of DIA monomer [40]) in the [- 3; - 7] ppm range, indicating that the free monomers all reacted to form oligomers, which confirmed the earlier results by Souguir *et al.* [13,14]. The integration of both deconvoluted D^1 and D^2 peaks indicated a $\overline{DP}_n$ of DIA in J4 treated with AP-DIA 5-95 about 14 at (t), which increased to 30 at (t + 3). T signals related to trifunctional AP in the [- 40; - 70] ppm range [40] were almost not noticeable, which could be attributed to its very low proportion in the treatment formulation (5 wt%). To investigate whether the assumption of neglecting the contribution of AP in the copolymer $\overline{DP}_n$ was correct, ^{29}Si CP-MAS NMR was carried out on C3a treated with DIA 100% (UP = 9 ± 3%, treatment by spray), at (t) and (t + 6). The integration of D^1 and D^2 yielded $\overline{DP}_n$ about 13 at (t) and 36 at (t + 6), values which are in agreement with those calculated for J4 treated with AP-DIA 5-95. Thus, the kinetics of polymerization of DIA in both papers was extremely slow, leading after several years to small oligomers. This confirms the hypothesis of very slow polycondensation kinetics, and is consistent with the increase of the hydrophobic character of the treated papers with time.

The average $\overline{DP}_n$ of AM in J4 treated with AP-AM 5-95 was about 36 at (t + 4), as shown by the ^{29}Si CP-MAS NMR spectrum (Figure S8 in the Supporting Information file). Thus, for a similar duration, the oligomerization of AM and DIA leads to a similarly low $\overline{DP}_n$. These temporal modifications of the $\overline{DP}_n$ of the AAAS in the paper may have an impact on its mechanical properties.

3.4. Mechanical properties changes

FE and TS measurements were carried out, which allowed obtaining N(FE), BL, EB and *Y* values for J4 and for the model papers. While TS measures the inter- and intra-fiber strength, FE is a wear test related to the flexibility of the paper, but also to its tensile strength, as the test specimen is under tension that eventually causes failure. FE is widely used for the evaluation of paper permanence as it is more sensitive to early modifications than tensile strength measurements, even though the data are less repeatable [41]. More than BL, EB provides information about the material's ductility, *i.e.* its ability to undergo plastic deformation before breaking. Young modulus *Y* is a measurement of the paper stiffness and elasticity.

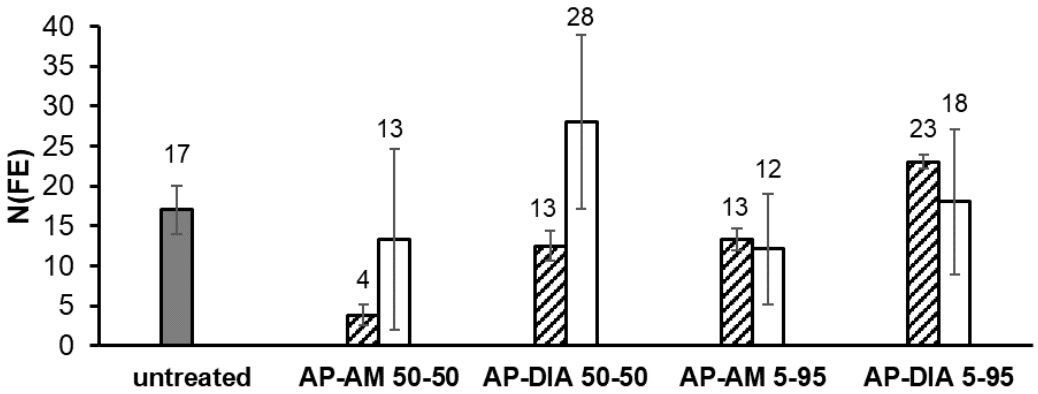

Figure 6. Number of double folds (N(FE)) of J4 treated with AP-AM and AP-DIA (50-50 and 5-95). Grey filled bar: J4 untreated (t_0). Hatched bars: J4 treated at (t). White bars: J4 treated at (t + 3) (UP is in Table S1).

At (t), AP-DIA 5-95 was the only formulation to improve FE of J4, even if only slightly, with average N(FE) = 23 compared to the initial value N(FE) = 17 (Figure 6). However, three years after, J4 treated with the 50-50 proportion of both AP-AM and AP-DIA showed an improved FE, with the highest N(FE) of 28 obtained with AP-DIA 50-50 at (t + 3). In contrast, when treated with the 5-95 formulation of either AP-AM or AP-DIA, FE did not significantly vary over time. This result pointed out that the strengthening effect of AP after several years was only observable for its highest proportion in the co-AAAS formulation. BL, EB and *Y* of J4 treated with AP-DIA 5-95 are in Figure 7 (no sample of J4 treated with AP-DIA 50-50 was available).

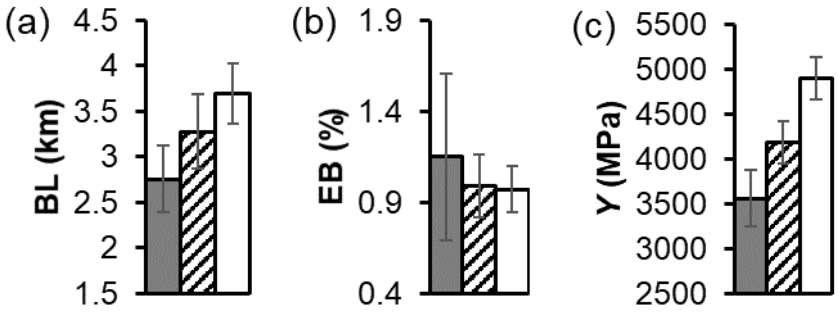

Figure 7. (a) Breaking Length (BL), (b) Elongation at Break (EB) and (c) Young modulus (*Y*) of J4 treated with AP-DIA 5-95. Grey filled bars: J4 untreated (t_0). Hatched bars: J4 treated at (t) (UP = 7 ± 1%). White bars: J4 treated at (t + 3) (UP = 6 ± 1%).

At (t), BL and *Y* increased (+ 19% and + 18%, respectively), while EB did not change significantly. In other words, J4 had a higher BL but also became stiffer (higher *Y*). In addition, BL and *Y* kept increasing between (t) and (t + 3) (+ 13% and + 17%, respectively) with still no change in EB.

The data at (t) and (t + x) of the model papers treated with AP-DIA 50-50 are shown in Figure 8 and Figure 9.

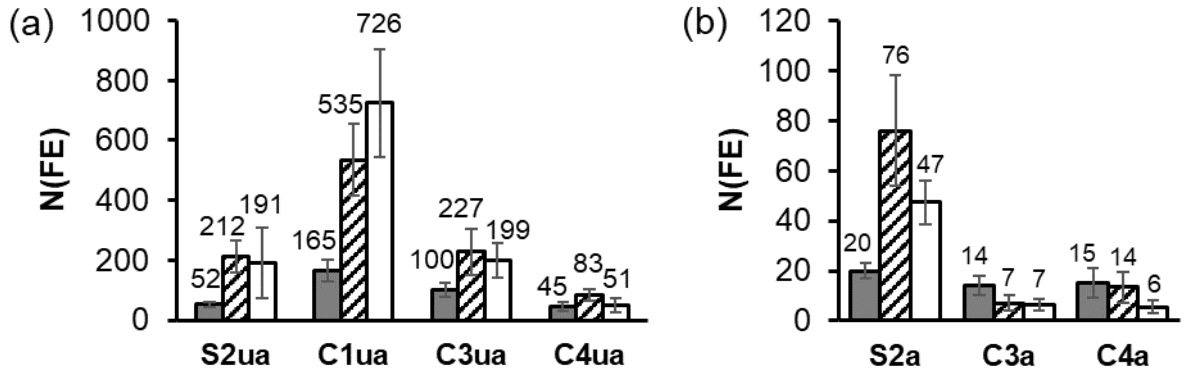

Figure 8. Number of double folds (N(FE)) of the model papers treated with AP-DIA 50-50. (a) unaged papers and (b) aged papers. Grey filled bar: untreated papers (t_0). Hatched bars: treated papers at (t) (data from Piovesan et *al.* 2017 and 2018 [14,15]). White bars: treated papers at (t + x) (x and UP are in Table S1).

Confirming previous findings [18,19], the application of AP-DIA 50-50 to the unaged model papers S2ua, C1ua, C3ua and C4ua and to the aged S2a improved FE at (t) to various levels (Figure 8). Besides C1ua, which showed a large increase of FE with time (+ 36%), the other papers showed FE at (t + x) that was either stable (S2ua and C3ua) or lower (C4ua, - 38%, S2a, - 38% and C4a, - 59%). Nevertheless, for S2a, N(FE) decreased from 76 at (t) to 47 at (t + x). However, this is still 2.4 times the value at (t_0) (N(FE) = 20). This indicates that FE strengthening of S2a, if not stable, at least was durable. For C3a and C4a, the treatment did not improve FE at (t), and a slight decrease occurred over time for C4a. N(FE) variations of the model papers treated with AP-AM 50-50 over time were very similar to those observed when treated with AP-DIA 50-50 (Figure S9 in the Supporting Information file).

BL of the model papers at (t) were all above the values at (t_0), if only slightly for C1ua (Figure 9a). This indicates that the treatment AP-DIA 50-50 was efficient to strengthen all the papers. In addition, besides C4ua and S2a, which showed a stable BL at (t) and (t + x), the other model papers underwent an increase in BL with time. This is consistent with the slow progress of the polycondensation. No correlation could be established between the variations of BL and FE.

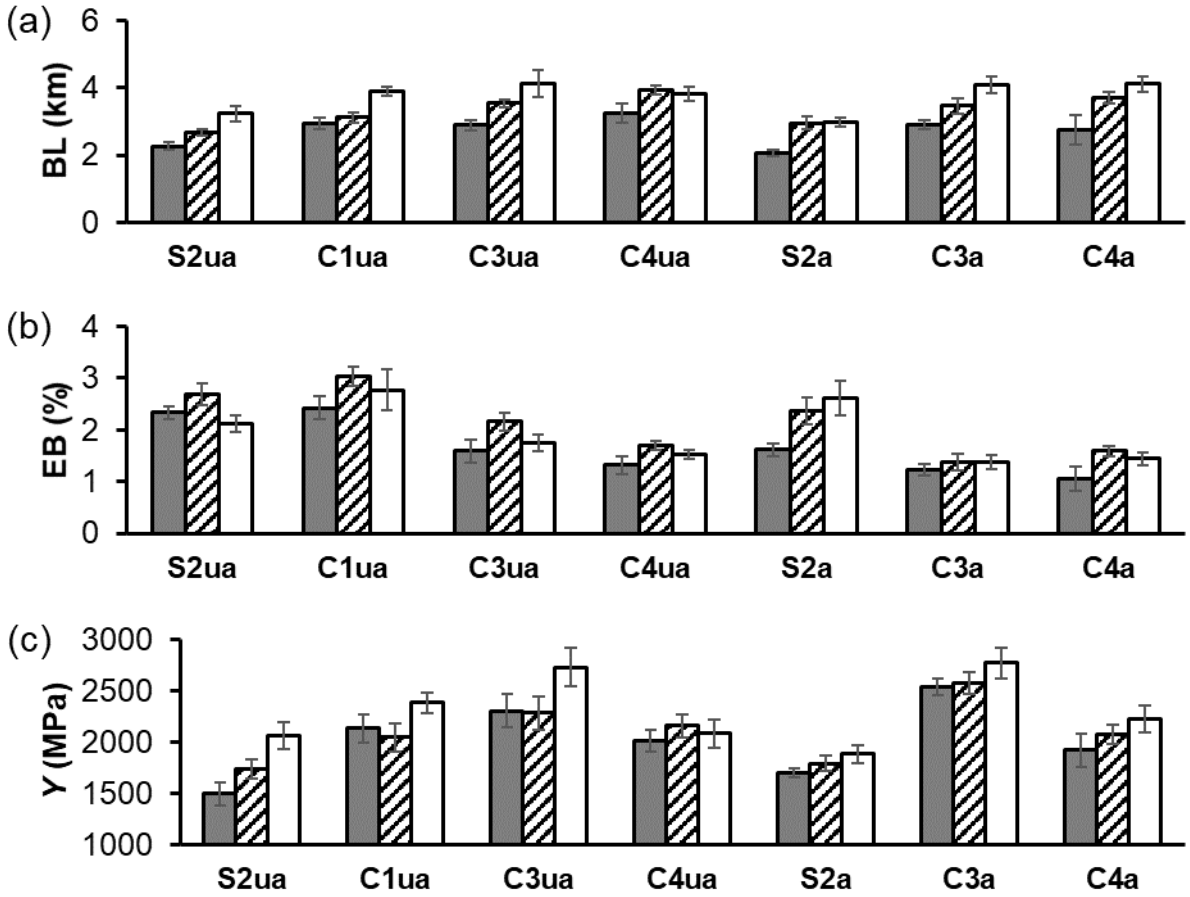

Figure 9. (a) Breaking Length (BL), (b) Elongation at Break (EB) and (c) Young modulus (*Y*) of the model papers (unaged and aged) treated with AP-DIA 50-50. Grey filled bars: untreated papers (t_0). Hatched bars: treated papers at (t). White bars: treated papers at (t + x) (x and UP are in Table S1).

The strengthening at (t) was observed with AP-AM 50-50 as well. Overall, at similar uptakes, BL values of the model papers were even higher than with AP-DIA 50-50 (Figure 10a). However, and except for C4ua, the opposite situation was observed at (t + x), where for each paper, ΔBL was higher with AP-DIA (Figure 10b). This is due to a larger decrease with time in BL of the papers treated with AP-AM, to the exception of C3a (Figure S10a). Nevertheless, for both formulations, at (t + x), BL values were always higher than at (t_0), which indicates a durable strengthening, despite the fluctuating temporal trends. In addition, at (t), with both formulations, the highest increase in BL was obtained for the sample with the highest uptake (Figure 10a). However, at (t + x), the absolute variation ΔBL was not proportional to the uptake (Figure 10b).

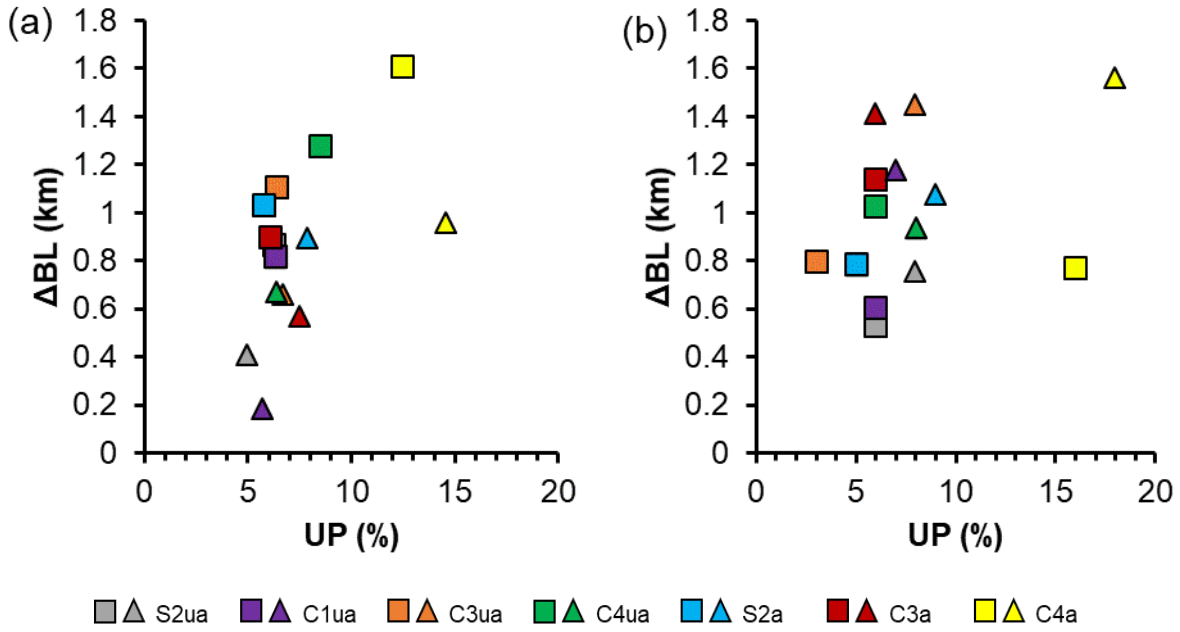

Figure 10. Absolute variation of breaking length (ΔBL) as a function of the uptake (UP) for the treated model papers (unaged and aged) at (a) (t) and (b) (t + x) (x is in Table S1). Squares: AP-AM 50-50. Triangles: AP-DIA 50-50.

At (t), EB of the model papers treated with AP-DIA 50-50 globally increased, if only slightly for C3a (Figure 9b). Between (t) and (t + x), EB evolved differently among the papers, and no correlation could be evidenced, neither with the constituents, nor with the increase in the $\overline{DP}_n$ of the AAAS. Besides, for the same formulation, the highest values of Y were those at (t + x) in all cases, where Y was higher than at (t_0), and also higher than at (t) (Figure 9c), showing that Y increased as the polycondensation of the AAAS progressed. Only C4ua did not follow this trend, as Y was similar at (t_0) (Y = 2008 ± 106 MPa), at (t) (Y = 2157 ± 110 MPa) and at (t + x) (Y = 2082 ± 137 MPa). Therefore, the stiffness of the treated papers increased with time, except for C4ua where it remained almost unchanged. This can be paralleled to the increase in Y observed for J4 treated with AP-DIA 5-95 (Figure 7c).

EB and Y of the model papers treated with AP-AM 50-50 are in Figures S10b and S10c (Supporting Information file). The absolute variations ΔEB and ΔY as a function of the uptake were plotted. For each paper, at similar uptakes, the application of AP-DIA induced higher ΔEB values, at (t) but also at (t + x) (Figure S11). In contrast, ΔY was overall higher at (t) and (t + x) with AP-AM 50-50 (Figure S12). Thus, ultimately, at (t + x), AP-DIA 50-50 led to higher BL and EB, whereas, as reported above, both AP-AM and AP-DIA yielded similar N(FE) (except for J4). Subsequently, and in contrast to the deacidification efficiency, in the 50-50 proportion, AP-DIA allowed a more sustainable strengthening of the paper than AP-AM.

Unlike with BL, no clear correlation was found with EB and Y when plotted as a function of the uptake at (t) and (t + x) (Figure S13 in the Supporting Information file). The variation of N(FE) as a

function of EB was investigated for AP-AM and AP-DIA. The relative variation of double folds ΔN was defined as follows:

$$\Delta N\ (\%) = \frac{N(FE)_a - N(FE)_b}{N(FE)_b} \times 100 \qquad (3)$$

where $N(FE)_a$ is the value after treatment (at (t) or (t + x)) and $N(FE)_b$ the value at (t_0). Figure 11a, which plots ΔN vs EB_a (EB after treatment), clearly shows that a larger increase of N(FE) was obtained for the papers which had the highest EB_a, whether at (t) or at (t + x). Conversely, negative values of ΔN were obtained for the samples with the lowest EB_a, indicating an embrittlement of the paper. The data point C4ua treated with AP-AM 50-50 at (t) was the only exception, as a significant improvement of FE, with ΔN of 237%, matched a low EB_a (EB_a = 1.53%). Even if the spread of the data set should be taken into consideration, ΔN and EB_a are otherwise strongly correlated. Moreover, as shown on Figure 11b, lower EB_b (EB before treatment) values were also correlated with lower ΔN. In other words, the increase in FE correlates with EB both before and after treatment. ΔN of S2ua and C1ua were high (157% < ΔN < 340%) because EB_b values were high (2.3% < EB_b < 2.5%). Conversely, an improvement in FE failed to occur for C3a and C4a (-71% < ΔN < -10%) as their EB_b were the lowest (1.0% < EB_b < 1.3%). On the other hand, no relevant relationship between ΔN and *Y* (before and after treatment) could be established at (t) and (t + x), indicating that *Y* and FE are not correlated (Figure S14 in the Supporting Information file).

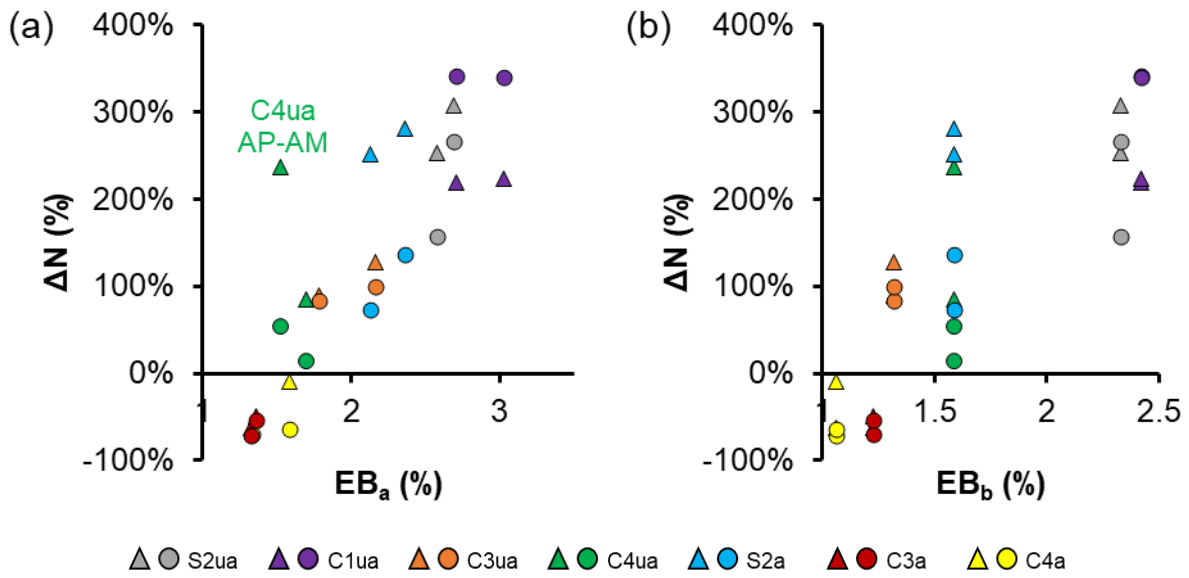

Figure 11. Relative variation of the number of double folds (ΔN) as a function of (a) EB_a (elongation at break after treatment) and (b) EB_b (elongation at break before treatment) for the model papers (unaged and aged) treated with AP-AM 50-50 and AP-DIA 50-50. Triangles: treated papers at (t). Circles: treated papers at (t + x) (x and UP are reported in Table S1).

While TS was always improved after treatment, the variations of FE depended considerably on the type of paper. Different trends were observed at (t), but also between (t) and (t + x). Firstly, FE was affected by the papers' constituents, independently of the degradation level (aged or unaged). C4ua was strengthened at (t), but N(FE) values at (t_0) and (t + x) were almost equal, showing that the FE strengthening was not sustained after several years. The lowest ΔN were obtained for the two papers with the lowest initial values, *i.e* the most degraded (aged) ones, C3a and C4a. As C4 is unsized, and because ΔN for C1ua, which is sized, was very high (ΔN = + 340%), it seems that the presence of alum-rosin was not a key factor of FE lack of strengthening. On the other hand, unaged alum-rosin differs chemically from aged alum-rosin. However, the alum-rosin sizing alone still does not explain why C4a (unsized) was not strengthened. The type of pulp and the fiber source seem more relevant. Among the most degraded papers, the lignin-rich groundwood pulp papers yielded ΔN values among the lowest. For instance, N(FE) of C4ua decreased further with time (ΔN = - 38%) than N(FE) of C3ua (ΔN = - 12%), and this was paralleled to the fact that the proportion of groundwood pulp is larger in C4 than in C3 (see Table 1). As described above, it was shown that the AAAS can react with acidic and oxidized functions, which are abundant in lignin and its degradation products [32]. It was hypothesized that these side reactions could affect the strengthening efficiency, especially in the case of the aged papers, which are more strongly oxidized. Indeed, the lignin-rich and very brittle (degraded) newsprint paper was the only paper to show no FE improvement after the addition of AP-DIA 5-95. In research by Souguir *et al.* where DIA was used to treat model papers and extremely brittle book sheets made of woodpulp [14], lignin-rich groundwood pulp and the fiber oxidation state were put forth as the main factors affecting the strengthening efficiency. The results obtained in the present work fully corroborated this hypothesis.

4. Conclusion

A temporal analysis of the physico-chemical properties of several papers treated with co-AAAS was undertaken. The first aim was to study the changes occurring with time, and hence the stability of the treatment and that of the treated paper. The second aim was to better understand the limiting factors in the durability of the deacidification and strengthening. To this purpose, the use of model papers was fully relevant in order to discriminate the respective contributions of the paper constituents. Alum was found to be the main possible cause of the progressive pH decrease of the most degraded treated papers with time. An alkaline reserve was consistently introduced in all the papers regardless of their composition and degradation state. This alkaline reserve started to be consumed within a few years after treatment in the most degraded papers sized with alum-rosin, showing how fast-decaying these papers are. Among the paper constituents, lignin was proven to affect the strengthening efficiency of the co-AAAS treatment the most, which corroborated previous observations and hypotheses. Upon treatment, the yellowing was also more pronounced in the papers containing alum-rosin sizing and/or lignin. The choice of the AAAS monomers was impactful as well. While AP-AM 50-50 was found more efficient

for a durable deacidification, the use of DIA instead of AM in the binary mixture with AP ultimately induced a more durable strengthening. It has to be noted that the time scale used in this temporal study was much shorter than the ''archival'' time scale. In order to examine the longer-term durability of the co-AAAS treatments, the monitoring should be continued in the future. As evidenced by ^{29}Si solid-state NMR, *in situ* polycondensation of the AAAS in the papers was shown to progress at a very slow pace in ambient conditions and evolved over the course of several years. Thus, the polymerization kinetics are also a key factor affecting the strengthening. In the future, the use of catalysts to speed up the polycondensation rate is conceivable in order to optimize the treatment formulation according to the paper constituents.

Acknowledgments

This work was supported by the Paris Seine Graduate School Humanities, Creation, Heritage, Investissements d'Avenir ANR-17-EURE-0021 – Foundation for Cultural Heritage Science, and by the Ile-de-France DIM RESPORE. The participation of the Bibliothèque Nationale de France is acknowledged. Alice Gimat and Oulfa Belhadj (CRC), Isabelle Fabre-Francke and Sophie Cantin (LPPI), Hervé Cheradame (Polytheragene), Mohamed Haouas and Nathalie Steunou (Institut Lavoisier de Versailles) are warmly thanked for technical contribution and fruitful discussions.

A Supplementary Material file is available. It contains supporting information to the article, including the values of UP and the aging duration x, ATR-FTIR spectrum (J4, (t_0)) titration curves (pH = f(V)) of AP, AM and DIA, ^{29}Si NMR spectrum (J4 treated with AP-AM 5-95, (t + 4)), and pH, b^*, opacity, N(FE), BL, EB and Y values of the treated papers.

References

[1] W.J. Barrow, Permanence/Durability of the Book VII. Physical and Chemical Properties of Book Papers 1507-1949, ERIC. (1974) 1–48.
[2] G.A. Smook, Handbook for Pulp & Paper Technologists, Michael Kocurek, TAPPI, Vancouver, 1982.
[3] E. Adler, Lignin chemistry - Past, present and future, Wood Sci. Technol. 11 (1977) 169–218. https://doi.org/10.1007/BF00365615.
[4] C. Heitner, The Photochemistry of Lignin, in: Taylor & Francis, Boca Raton, 2010: pp. 555–584. https://doi.org/10.1201/EBK1574444865-c16.
[5] M. Paulsson, J. Parkås, Review: Light-Induced Yellowing of Lignocellulosic Pulps - Mechanisms and Preventive Methods, BioResources. 7 (2012) 5995–6040. https://doi.org/10.15376/biores.7.4.5995-6040.
[6] J.C. Williams, A Review of Paper Quality and Paper Chemistry, Library Trends. (1981) 203–224.
[7] M.C. Area, H. Cheradame, Paper aging and degradation: recent findings and research methods, BioResources. 6 (2011) 5307–5337. https://doi.org/10.15376/biores.6.4.5307-5337.

[8] M. Jablonsky, J. Šima, M. Lelovsky, Considerations on factors influencing the degradation of cellulose in alum-rosin sized paper, Carbohydrate Polymers. 245 (2020) 116534. https://doi.org/10.1016/j.carbpol.2020.116534.
[9] H.A. Carter, The Chemistry of Paper Preservation: Part 1. The Aging of Paper and Conservation Techniques, J. Chem. Educ. 73 (1996) 417–420. https://doi.org/10.1021/ed073p417.
[10] J.W. Baty, C.L. Maitland, W. Minter, M.A. Hubbe, S.K. Jordan-Mowery, Deacidification for the conservation and preservation of paper-based works: a review, BioResources. 5 (2010) 1955–2023. https://doi.org/10.15376/biores.5.3.1955-2023.
[11] H. Cheradame, S. Ipert, E. Rousset, Mass Deacidification of Paper and Books. I: Study of the Limitations of the Gas Phase Processes, Restaurator. 24 (2003) 227–239. https://doi.org/10.1515/REST.2003.227.
[12] A.-L. Dupont, B. Lavédrine, H. Cheradame, Mass deacidification and reinforcement of papers and books VI–Study of aminopropylmethyldiethoxysilane treated papers, Polymer Degradation and Stability. 95 (2010) 2300–2308.
[13] Z. Souguir, A.-L. Dupont, J.-B. d'Espinose de Lacaillerie, B. Lavédrine, H. Cheradame, Chemical and Physicochemical Investigation of an Aminoalkylalkoxysilane As Strengthening Agent for Cellulosic Materials, Biomacromolecules. 12 (2011) 2082–2091. https://doi.org/10.1021/bm200371u.
[14] Z. Souguir, A.-L. Dupont, K. Fatyeyeva, G. Mortha, H. Cheradame, S. Ipert, B. Lavédrine, Strengthening of degraded cellulosic material using a diamine alkylalkoxysilane, RSC Advances. 2 (2012) 7470–7478. https://doi.org/10.1039/c2ra20957h.
[15] S.E. Rankin, A.V. McCormick, Hydrolysis pseudoequilibrium: challenges and opportunities to sol–gel silicate kinetics, Chemical Engineering Science. 55 (2000) 1955–1967. https://doi.org/10.1016/S0009-2509(99)00486-8.
[16] M.-C. Brochier Salon, P.-A. Bayle, M. Abdelmouleh, S. Boufi, M.N. Belgacem, Kinetics of hydrolysis and self condensation reactions of silanes by NMR spectroscopy, Colloids and Surfaces A: Physicochemical and Engineering Aspects. 312 (2008) 83–91. https://doi.org/10.1016/j.colsurfa.2007.06.028.
[17] C. Piovesan, A.-L. Dupont, I. Fabre-Francke, O. Fichet, B. Lavédrine, H. Cheradame, Paper strengthening by polyaminoalkylalkoxysilane copolymer networks applied by spray or immersion: a model study, Cellulose. 21 (2014) 705–715. https://doi.org/10.1007/s10570-013-0151-9.
[18] C. Piovesan, I. Fabre-Francke, A.-L. Dupont, O. Fichet, S. Paris-Lacombe, B. Lavédrine, H. Cheradame, The impact of paper constituents on the efficiency of mechanical strengthening by polyaminoalkylalkoxysilanes, Cellulose. 24 (2017) 5671–5684. https://doi.org/10.1007/s10570-017-1513-5.
[19] C. Piovesan, I. Fabre-Francke, S. Paris-Lacombe, A.-L. Dupont, O. Fichet, Strengthening naturally and artificially aged paper using polyaminoalkylalkoxysilane copolymer networks, Cellulose. 25 (2018) 6071–6082. https://doi.org/10.1007/s10570-018-1955-4.
[20] J. Wittekind, The Battelle Mass Deacidification Process: a New Method for Deacidifying Books and Archival Materials, Restaurator. 15 (1994) 189–207. https://doi.org/10.1515/rest.1994.15.4.189.
[21] I.H. Isenberg, Pulp and paper microscopy, 3rd ed., Institute of Paper Chemistry, 1967.
[22] B.L. Browning, Analysis of Paper, Enlarged 2nd edition, M. Dekker, New York, 1977.
[23] M. Derrick, D. Stulik, J.M. Landry, Infrared Spectroscopy in Conservation Science, Getty Conservation Institute, Los Angeles, 1999.
[24] D. Massiot, F. Fayon, M. Capron, I. King, S. Le Calvé, B. Alonso, J.-O. Durand, B. Bujoli, Z. Gan, G. Hoatson, Modelling one- and two-dimensional solid-state NMR spectra: Modelling 1D and 2D solid-state NMR spectra, Magnetic Resonance in Chemistry. 40 (2002) 70–76. https://doi.org/10.1002/mrc.984.
[25] T. Cabaret, B. Boulicaud, E. Chatet, B. Charrier, Study of rosin softening point through thermal treatment for a better understanding of maritime pine exudation, European Journal of Wood and Wood Products. 76 (2018) 1453–1459. https://doi.org/10.1007/s00107-018-1339-3.
[26] J.S. Mills, R. White, The Organic Chemistry of Museum Objects, Butterworth-Heinemann, 1994.
[27] G. Banik, I. Bruckle, Paper and Water: A Guide for Conservators, 1st ed., Butterworth-Heinemann, Amsterdam; New York, 2011.

[28] J.M. Gess, The sizing of paper with rosin and alum at acid pHs, in: J.C. Roberts (Ed.), Paper Chemistry, Springer Netherlands, Dordrecht, 1996: pp. 120–139. https://doi.org/10.1007/978-94-011-0605-4_8.
[29] V. Bukovský, Yellowing of Newspaper after Deacidification with Methyl Magnesium Carbonate, Restaurator. 18 (1997) 25–38. https://doi.org/10.1515/rest.1997.18.1.25.
[30] C. Piovesan, I. Fabre-Francke, T.-P. Nguyen, C.S. Grimoüard, O. Fichet, A.-L. Dupont, Application de traitements à base de polyaminoalkylalcoxysilanes pour la désacidification et le renforcement simultanés de documents anciens sur papier, Support Tracé. (2018) 106–116.
[31] R. Sève, Physique de la couleur : de l'apparence colorée à la technique colorimétrique, Dunod, Paris, 1997.
[32] N. Ferrandin-Schoffel, M. Haouas, C. Martineau-Corcos, O. Fichet, A.-L. Dupont, Modeling the Reactivity of Aged Paper with Aminoalkylalkoxysilanes as Strengthening and Deacidification Agents, ACS Appl. Polym. Mater. 2 (2020) 1943–1953. https://doi.org/10.1021/acsapm.0c00132.
[33] W.M. Bundy, J.N. Ishley, Kaolin in paper filling and coating, Applied Clay Science. 5 (1991) 397–420. https://doi.org/10.1016/0169-1317(91)90015-2.
[34] K. Balani, V. Verma, A. Agarwal, R. Narayan, Physical, Thermal, and Mechanical Properties of Polymers, in: Biosurfaces: A Materials Science and Engineering Perspetive, John Wiley & Sons, Ltd, 2015: pp. 329–344. https://doi.org/10.1002/9781118950623.app1.
[35] J. Brus, J. Dybal, Solid-state NMR study of structure, size and dynamics of domains in hybrid siloxane networks, Polymer. 41 (2000) 5269–5282. https://doi.org/10.1016/S0032-3861(99)00741-7.
[36] M. Cypryk, Y. Apeloig, Mechanism of the Acid-Catalyzed Si–O Bond Cleavage in Siloxanes and Siloxanols. A Theoretical Study, Organometallics. 21 (2002) 2165–2175. https://doi.org/10.1021/om011055s.
[37] C. Daher, I. Fabre-Francke, N. Balcar, G. Barabant, S. Cantin, O. Fichet, H. Chéradame, B. Lavédrine, A. Lattuati Derieux, Consolidation of degraded polyurethane foams by means of polysiloxane mixtures: Polycondensation study and application treatment, Polymer Degradation and Stability. 158 (2018) 92–101. https://doi.org/10.1016/j.polymdegradstab.2018.10.029.
[38] E. Pellizzi, A. Lattuati-Derieux, J.-B. d'Espinose de Lacaillerie, B. Lavédrine, H. Cheradame, Reinforcement properties of 3-aminopropylmethyldiethoxysilane and N-(2-Aminoethyl)-3-aminopropylmethyldimethoxysilane on polyurethane ester foam, Polymer Degradation and Stability. 97 (2012) 2340–2346. https://doi.org/10.1016/j.polymdegradstab.2012.07.031.
[39] J. Rocha, J. Klinowski, 29Si and 27Al magic-angle-spinning NMR studies of the thermal transformation of kaolinite, Phys Chem Minerals. 17 (1990) 179–186. https://doi.org/10.1007/BF00199671.
[40] S. de Monredon-Senani, Interaction Organosilanes/Silice de précipitation Du milieu hydro-alcoolique au milieu aqueux, thesis, Paris 6, 2004. http://www.theses.fr/2004PA066195 (accessed February 5, 2019).
[41] E. Princi, Handbook of Polymers in Paper Conservation, Smithers Rapra, 2011.